Journal of Seismology (2005) **9:** 295–316 

# Treatment of ground-motion predictive relationships for the reference seismic hazard map of Italy

Valentina Montaldo[1,*], Ezio Faccioli[2], Gaetano Zonno[1], Aybige Akinci[3] & Luca Malagnini[3]
[1]*Istituto Nazionale di Geofisica e Vulcanologia, Sezione "Sismologia Applicata", via Bassini 15, 20133, Milano, Italy;* [2]*Department of Structural Engineering, Politecnico di Milano, Piazza L. da Vinci 32, 20133 Milano, Italy;* [3]*Istituto Nazionale di Geofisica e Vulcanologia, Sezione "Sismologia e Tettonofisica", via di Vigna Murata 605, 00143, Roma, Italy*
[*]*Author for correspondence: e-mail: montaldo@mi.ingv.it*

Received 16 August 2004; accepted in revised form 20 April 2005

*Key words:* epicentral and Joyner-Boore distance, epistemic uncertainty, predictive relationships, seismic hazard mapping, scaling laws, volcanic regions

**Abstract**

In the framework of the 2004 reference seismic hazard map of Italy the amplitude of the strong-motion (expressed in terms of Peak Horizontal Acceleration with 10% probability of non-exceedence in 50 years, referred to average hard ground conditions) was computed using different predictive relationships. Equations derived in Italy and in Europe from strong-motion data, as well as a set of weak and strong-motion based empirical predictive relationships were employed in a logic tree procedure, in order to capture the epistemic uncertainty affecting ground-motion attenuation. This article describes the adjustments and conversions required to eliminate the incompatibilities amongst the relations. Particularly significant are distance conversions and style-of-faulting adjustments, as well as the problems related to the use of regional relations, such as the selection of a reference depth, the quantification of random variability and the strong-motion prediction. Moreover, a regional attenuation relationship specific for volcanic areas was also employed, allowing a more realistic evaluation of seismic hazard, as confirmed by the attenuation of macroseismic intensities.

## Introduction

Seismic hazard mapping based on the probabilistic Cornell-McGuire approach (Cornell, 1968; McGuire, 1976) is used worldwide as a tool for the application of seismic codes. In its more general formulation the Cornell-McGuire method assumes stationarity of the seismogenic process, modelled by a Poisson distribution of earthquake occurrences and by a uniform spatial distribution of events within source zones.

Some basic elements needed in a probabilistic analysis, such as earthquake source zones, maximum magnitude and ground-motion attenuation, do not differ from those required by a deterministic approach. However, the impact of the input assumptions in probabilistic seismic hazard analysis is less obvious and can be completely evaluated only after the computation is carried out and sensitivity tests are performed (Reiter, 1990).

Recent developments in probabilistic seismic hazard analysis explore the possibility of entering more than one model into the calculation, with the twofold purpose of reducing the influence of a single choice and of explicitly accounting for the epistemic uncertainty related to the lack of knowledge. This can be done through a logic tree, i.e. a flow chart the branches of which ought to represent mutually exclusive events and are assigned a likelihood of being correct (Kulkarni et al., 1984; Coppersmith and Youngs, 1986). Logic trees are particularly useful for assessing the ground-motions since a large number of attenuation relations are currently available for many regions in the world,

but the incompatibilities amongst such relations must be accounted for (Bommer et al., 2005).

This article describes the application of different ground-motion relations in the framework of the 2004 project leading to a new seismic hazard map of Italy. This map, required by the enforcement of a new seismic design code, was produced in less than one year and fulfilled the requirements stated by the law. In particular, the map is expressed in terms of Peak Horizontal Acceleration (*PHA*) with 10% probability of non-exceedance in 50 years, referred to average hard ground conditions, i.e. a weighted-average S-wave velocity in the uppermost 30 m ($Vs_{30}$) greater than 800 m/s.

The analysis was conducted using a 16-branches logic tree in which only one model was proposed for the seismic source zones and only one earthquake catalogue was adopted, while independent branches were introduced for the completeness intervals of the catalogue, for the frequency-magnitude relationships and for ground-motion attenuation (Gruppo di Lavoro MPS, 2004). The weighting scheme adopted in the logic tree accounts for sensitivity analysis and expert judgment. The seismic hazard map was constructed using the SEISRISK III (Bender and Perkins, 1987) computer code; the results were submitted for evaluation to a panel of reviewers and approved in April 2004.

The epistemic uncertainty affecting ground-motion attenuation has been tackled by four branches that consider the use of: (a) the Ambraseys et al. (1996) relation valid for Europe, (b) the Sabetta and Pugliese (1996) relation valid for Italy, and (c) a set of "regional" relations derived from regional seismicity (weak- and strong-motion data; the latter appears in two branches as will be discussed later). Particular care was devoted to the consistency of the magnitude and distance data with the definitions required by the different attenuation relations, in order to ensure that the final results be free from fundamental errors. Moreover, the application of recently proposed style-of-faulting adjustments (Bommer et al., 2003) and the introduction of regional attenuations (including one specific for volcanic areas), represent a step towards making a fuller use of the available geological and seismological knowledge, so far confined to the definition of source zones (at least in Italy).

In the first part of this article, a number of selected attenuation relations will be introduced and their characteristics briefly described. Since strong-motion based relationships pose different problems from weak-motion based relations, they will be discussed separately. The conversion of distances and the application of style-of-faulting adjustments are treated next, while the subsequent section deals with the regional relationships and related problems, such as the selection of a reference depth, the quantification of random variability and the strong-motion prediction. The regional relations used in volcanic areas are subsequently illustrated. Finally, the last section is devoted to the weighting scheme adopted for the attenuation branches of the logic tree.

## Predictive relationships available for Italy

The new Italian seismic code, consistently with Eurocode 8 (CEN, 2004), states that the seismic hazard map of the country must represent values of peak ground acceleration. As a consequence, only relations for peak acceleration attenuation have been taken into account. The ground-motion predictive relationships available for Italy include those of Sabetta and Pugliese (1987, in the following SP87), Tento et al. (1992, in the following TFM92), Ambraseys (1995, in the following AMB95), Ambraseys et al. (1996, in the following ASB96) and Sabetta and Pugliese (1996, in the following SP96). Additional relationships are available for the European region, e.g. Ambraseys and Bommer (1991a) and Tromans and Bommer (2002) that made use of data sets including many recordings form Italy.

SP87 has been derived from a data set of 95 Italian accelerograph records of 17 earthquakes with magnitude $M$ ranging between 4.6 and 6.8, where $M = M_L$ for $M < 5.5$, and $M = M_S$ for $M \geq 5.5$ in order to match the $M_W$ magnitude. SP87 takes two different forms, one as a function of epicentral distance, and the other as a function of the Joyner and Boore (1981) distance, i.e. the shortest distance from the surface projection of the fault. Both forms include site-specific coefficients.

A dataset similar to that used by SP87, has been employed to derive the TFM92 relation, defined for $4.0 \leq M_L \leq 6.6$. The distance adopted is the shortest distance to the fault, except for small events ($M_L < 5.7$) for which the epicentral distance is taken. TFM92 does not take site classification into account.

The AMB95 relation rests on a set of over 400 European strong-motion records of earthquakes with $4.0 \leq M_S \leq 7.4$. The reference magnitude is $M_S$, while distance is defined as either epicentral distance ($M_S < 6.0$) or Joyner-Boore distance (Joyner and Boore, 1981) for larger events. Like TFM92, the predictive relation is valid for a generic soil. AMB95 has been employed in the 1996 seismic hazard map of Italy

(Slejko et al., 1998) without introducing modifications to account for the non-unique distance definition.

The ASB96 relationship updates AMB95, the main differences being the introduction of site-specific coefficients and the addition of predictive relations for the response spectral ordinates (not discussed here). ASB96 uses the same magnitude scale and distance definition as AMB95 and has been used in seismic hazard mapping at global (Giardini, 1999), European (Jiménez et al., 2001) and national scale (Slejko et al., 1999; Albarello et al., 2000), in all cases neglecting the inconsistency between Joyner-Boore distance and the distance definition adopted by the computer code SEISRISK III (Bender and Perkins, 1987). Since the latter uses the distance from the site to a grid of points within the seismic source zone, the Joyner-Boore distance must be converted.

Finally, the predictive relation SP96 in terms of PHA is the same as SP87. It was used in seismic hazard mapping of Italy by Albarello et al. (2000) and by Romeo and Pugliese (2000), albeit improperly. In fact, while at that time the Italian earthquake catalogues were compiled for $M_S$ only, the latter studies give no indication as to whether the $M_S$ magnitudes were converted as required by SP96 for $M < 5.5$.

Based on this information, ASB96 and SP96 were adopted for the new seismic hazard map because the respective calibration datasets contain all the most important strong-motion records available from Italian earthquakes.

Currently, a set of empirical predictive relationships is available for different geographical regions of Italy, which were derived from the regional data (weak- and strong-motion databases), containing thousands of waveforms recorded in areas with homogeneous attenuation characteristics (Malagnini and Herrman, 2000; Malagnini et al., 2000, 2002; Morasca et al., 2002). As an example, Malagnini et al. (2000) used strong-motion data from the $M_W$ 6.0 event occurred in 1997 in the Colfiorito area, together with all the shocks of the sequence with $M_W > 5.5$. Moreover, for the regression analysis in the Eastern Alps region, Malagnini et al. (2002) gathered the entire strong-motion data set available (including the $M_W$ 6.5 Friuli event of 1976, the $M_W$ 5.5 event of 1977, and all their strongest aftershocks), together with a large set of regional weak-motion recordings.

Before introducing these relations in the logic tree procedure, the compatibility of the dependent (peak ground acceleration) and the independent variables (magnitude, distance and site class) must be granted amongst the relations and between the relations and the computational algorithm (Bommer et al., 2005). As to the dependent variable, all chosen relations use the largest peak horizontal component of motion. Consistency in the independent variables is much more complex to achieve. For magnitude, one can either produce an earthquake catalogue with different magnitude estimates for each earthquake, or apply magnitude conversions to adjust the predictive relations. For Italy the first option was preferred, and three different magnitudes were provided in the catalogue (Gruppo di Lavoro MPS, 2004). The problem of consistency in distance definitions will be discussed in detail in the next section, together with the introduction of style-of-faulting adjustments.

Finally, the Italian seismic code (consistently with Eurocode 8) states that the seismic hazard map represents ground acceleration on hard ground sites, i.e. sites with $Vs_{30} > 800$ m/sec. The adopted attenuation relations use a similar ground classification: rock or very stiff soil is defined by $Vs_{30} > 760$ m/s in ASB96, while it corresponds to outcropping rock with $V_S > 800$ m/s in SP96. Similar definitions are valid also for the regional attenuation relations.

Table 1 summarises the main characteristics of the adopted attenuation relations highlighting the most important adjustments and conversions introduced.

## Strong-motion based attenuation relations: Conversions and adjustments

In this section, we illustrate the development and the application of distance conversion relations and style-of-faulting adjustments to ASB96 and SP96.

### *Distance conversion relations*

ASB96 uses a non-unique definition of distance based on the observation that large earthquakes are usually generated by fault segments of finite dimensions, while minor events are generated by smaller faults that can be approximated by point sources.

In the SEISRISK III code (Bender and Perkins, 1987) seismic source zones, assumed at zero depth, are subdivided into a grid of points representing the possible locations of an earthquake and then the geometric distance between each "earthquake location" and the site is computed. This distance is used to attenuate the ground-motion. Epicentral distance measures the distance between a site and the surface projection of the earthquake's hypocenter,

*Table 1*. Main characteristics of the adopted attenuation relationships. Abbreviations indicate the type of records: (a) accelerogram; (bb) broad band data; and (s) seismogram

| | | | Regionalized relations | | | |
|---|---|---|---|---|---|---|
| Item | ASB96 | SP96 | REG 1 | REG 2 | REG 3 | REG 4 |
| Component of motion | Largest horizontal | Largest horizontal | Largest horizontal | Largest horizontal | Largest horizontal | Largest horizontal |
| Number of waveforms | 422 (a) | 95 (a) | >7500 (bb) | 6982 (s + a) | >6000 (s) | ~170(s) |
| Magnitude range | $4 \leq M_S \leq 7.5$ | $4.6 \leq M^* \leq 6.8$ | $0.5 \leq M_L^* \leq 5.1$ | $1.0 \leq M_W \leq 6.1$ | $2.0 \leq M_W \leq 6$ | $0.7 \leq M_L^{**} \leq 3.5$ |
| Distance | Epicentral (converted for $M_S \geq 6$) | Epicentral | Epicentral (converted) | Epicentral (converted) | Epicentral (converted) | Epicentral (converted) |
| Distance range [km] | $R < 200$ | $R < 100$ | $R < 160$ | $20 \leq R \leq 200$ | $R < 200$ | $3 \leq R \leq 6$ |
| Style-of-faulting adjustments | Yes | Yes | No | No | No | No |
| Rock class [m/s] | $Vs_{30} > 760$ | $Vs > 800$ | $Vs_{30} > 800$ | $Vs_{30} > 800$ | $Vs_{30} > 800$ | $Vs_{30} > 800$ |
| Standard deviation ($\sigma_{\log y}^{***}$) | 0.25 | 0.19 | 0.20 | 0.20 | 0.20 | 0.20 |

*Sabetta and Pugliese assumed $M = M_L$ for $M < 5.5$ and $M = M_S$ for $M \geq 5.5$.
**Assumed equal to $M_W$ in the hazard calculations.
***The predictive relation is for the logarithm of the ground-motion parameter $y$.

i.e. the distance between two points located on the Earth's surface, therefore it can be considered the best approximation of the "geometric" distance used in SEISRISK III.

What happens then if we apply ASB96 in SEISRISK III, without correcting the distance? Since Joyner-Boore distance is always smaller than epicentral distance (except for the special case of a station located at the epicentre), the effect is that of underestimating the ground-motion. Some tests showed that in the case of Italy such underestimation can be as high as 20% of *PHA* for 475 years return period.

Our first trial to obtain a suitable distance conversion was to use well-known relations (Wells and Coppersmith, 1994) to determine fault dimensions for earthquakes of magnitude $M_S \geq 6.0$. Then, assuming a simple geometry with the epicentre situated in the centre of mass of the fault and considering a single site arbitrarily located, we converted Joyner-Boore distance to epicentral distance. The results obtained were not satisfactory, probably because this model does not account for the depth distribution and for the position of the hypocenters on the fault plane (as in Scherbaum et al., 2004). The necessary refinements could not be explored due to the tight time schedule of the project.

As a second alternative, the SP96 relationships for fault and for epicentral distance have been used. For a given magnitude, imposing equality among the two relations and solving for distance yields:

$$R_{JB} = \left[\left(R_{EPI}^2 + 25\right)10^{0.566-0.114M} - 5.8^2\right]^{1/2} \quad (1)$$

where $R_{JB}$ is the Joyner and Boore (1981) distance, $R_{EPI}$ is the epicentral distance and $M = M_S$.

On the same line of reasoning, we also derived a conversion relation using the information provided in the European Strong-Motion Database (Ambraseys et al., 2004; available online at the URL: http://www.isesd.cv.ic.ac.uk/) containing data recorded in Europe and the Near East, and the strong-motion database by Ambraseys and Bommer (1991b).

The very recent Ambraseys et al. (2004) database contains more than 3000 uniformly processed accelerograph recordings, among which 785 Italian records have been retrieved. However, measures of epicentral and Joyner-Boore distance are available for less than 100 of these records, while in the Ambraseys and Bommer (1991b) database the same distance measures are provided for 164 European records.

We have performed two different regression analysis using in one case only the Italian data, and in the other the data from Europe. The resulting distance

conversion relationships are:

$$R_{JB} = -5.0497 + 0.9433 R_{EPI}$$
(Italian data, from Ambraseys et al., 2004) (2)

$$R_{JB} = -3.5525 + 0.8845 R_{EPI}$$
(European data, from Ambraseys and Bommer, 1991b) (3)

The values of $R^2$ (correlation coefficient) are extremely good, respectively 0.98 for Eq.2 and 0.95 for Equation (3).

In Figure 1 are compared the curves obtained using Equation (1) (for $M_S6$ and $M_S7$, respectively the dashed and solid thin lines), Equation (2) (dotted black line) and Equation (3) (solid black line). The results of Equation (1) are not completely reliable at short distances because the records in SP96 database are mainly distributed at distances greater than 10 km. This is shown in the figure, where the two curves have a non-linear trend from 1 to 15 km. Moreover, since the source dimensions play a role only at relatively short distance (15–30 km, depending on magnitude) the two curves should not diverge at large distances. For these reasons, Equation (1) was disregarded even though it has the advantage of being magnitude dependent. The curves obtained from Equation (2) and Equation (3) show a similar behaviour. The choice among these two relations is guided by the fact that some errors were found in the Ambraseys et al. (2004) database, in particular for 12 records the Joyner-Boore distance value indicated is greater than the epicentral distance. Since the Ambraseys and Bommer (1991b) data seemed to be more reliable, it was finally decided to adopt the conversion of Equation (3). Moreover, the corresponding curve shown in Figure 1 seems to represent an average behaviour and shows also a good agreement with the conversions developed by Scherbaum et al. (2004, in grey: dashed lines for $M6$ and solid for $M7$).

Distance is corrected only for the larger earthquakes ($M_S \geq 6$), while for the smaller events the ASB96 predictive relation remains unchanged, i.e.:

$$\mathrm{Log}\left(PHA_{[g]}\right) = -1.48 + 0.266 M_S - 0.922 \mathrm{Log}([(-3.5525 + 0.8845 R_{EPI})^2 + 3.5^2]^{1/2}) \pm 0.25 \quad M_S \geq 6 \quad (4)$$

$$\mathrm{Log}\left(PHA_{[g]}\right) = -1.48 + 0.266 M_S - 0.922 \mathrm{Log}\left(\left[R_{EPI}^2 + 3.5^2\right]^{1/2}\right) \pm 0.25 \quad M_S < 6 \quad (5)$$

Equation 3 shows that if epicentral distance is smaller than 3.5 km, the Joyner-Boore distance will be negative, meaning that the point to which distance is measured lies within the fault projection on the surface. In this case the Joyner-Boore distance is assumed to be zero. Figure 2 shows the corrected (solid lines) and

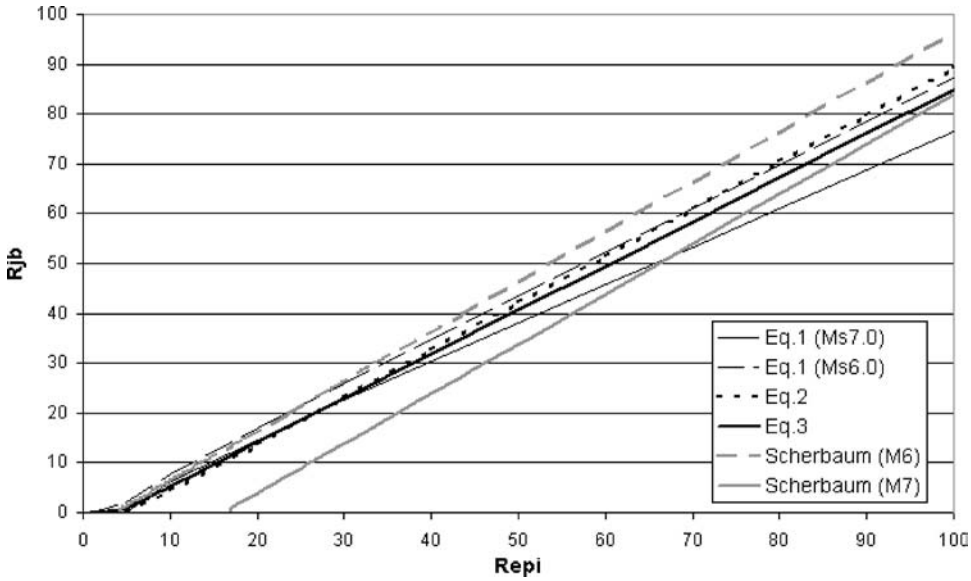


*Figure 1.* Comparison between different conversion relations.

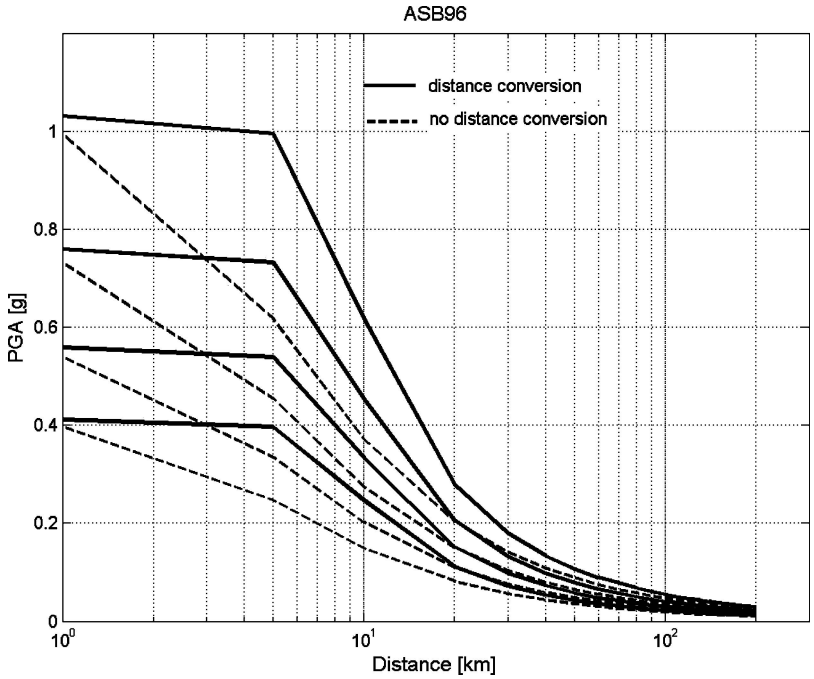


*Figure 2.* ASB96 as a function of epicentral distance, for $M_S \geq 6.0$. *Dashed lines* represent the original ASB96 curves for Joyner–Boore distance.

uncorrected (dashed lines) curves for $M_S \geq 6.0$. Using Equation (3) is an approximate way of accounting for the distance correction, but it satisfied the criteria of efficiency and rapidity in the application considering the time constraints imposed.

*Style-of-faulting adjustments*

It has often been recognized that style-of-faulting influences ground-motion, although only few predictive relations (mainly for US) take also this parameter into account. Recently, Bommer et al. (2003) analysed a number of strong-motion predictive relationships and proposed a simple method to scale any such relation according to style-of-faulting.

These authors inferred from published studies that, generally, the ratio of ground shaking amplitude produced by reverse faults compared to the average prediction is about 1.2 ($\pm$0.1), while normal faults tend to produce lower ground-shaking for a given magnitude and distance, with an average ratio of 0.95 ($\pm$0.05). Faults are classified according to the rake angle into three categories: "reverse", "normal" or "strike-slip". The method assumes that the distribution of residuals of individual mechanism-dependent sub-sets is equal to that of the overall equation. Three multiplicative factors, corresponding to the ratio between the ground-motion produced by earthquakes with a given fault mechanism to the ground-motion predicted by the overall distribution, are calculated. The standard deviation of the prediction equation was found not to be appreciably reduced by including the style-of-faulting coefficients.

Using the equations and the coefficients provided in Bommer et al. (2003; see their Equations (7a), (7b) and (7c); Tables 4 and 6), we computed the fault-style scaling factors for both ASB96 and SP96. The results are given in Table 2, where $p_N$ and $p_R$ are probabilities accounting for the number of normal ($N$) or reverse ($R$) fault earthquakes included in the database, while $F_{R:EQ}$, $F_{N:EQ}$ and $F_{SS:EQ}$ are the ratios between ground-motion produced by a given type of fault and the ground-motion predicted by the overall distribution

*Table 2.* Style-of-faulting coefficients for ASB96 and SP96: $p_N$ and $p_R$ are probabilities; $F_{R:EQ}$, $F_{N:EQ}$ and $F_{SS:EQ}$ are the scaling coefficients respectively for reverse, normal and strike-slip faulting

| Predictive relation | $p_N$ | $p_R$ | $F_{R:EQ}$ | $F_{N:EQ}$ | $F_{SS:EQ}$ |
|---|---|---|---|---|---|
| Ambraseys et al. (1996) | 0.3069 | 0.4455 | 1.13 | 0.88 | 0.93 |
| Sabetta and Pugliese (1996) | 0.4988 | 0.4410 | 1.15 | 0.89 | 0.94 |

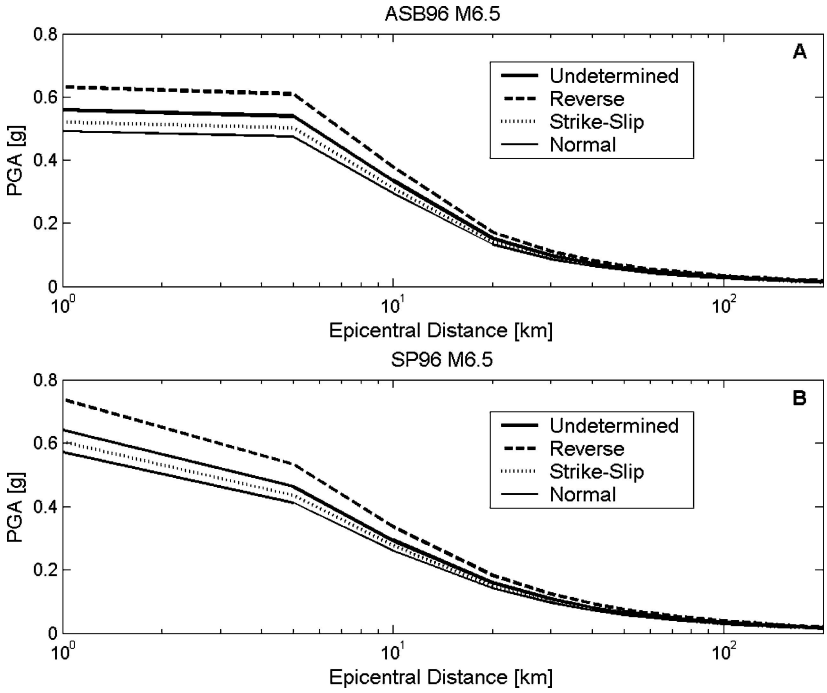


*Figure 3*. Style-of-faulting adjustments: (a) ASB96 for $M_S$ 6.0; (b) SP96 for $M_S$ 6.0.

(*EQ*); the symbols *N*, *R* and *SS* refer respectively to normal, reverse and strike-slip faults.

Since the application of these coefficients into seismic hazard assessment requires the definition of a predominant style-of-faulting for each of the source zones, a map of predominant style-of-faulting was prepared by Gruppo di Lavoro MPS (2004) for the purpose, looking at the prevalent focal mechanism and considering all the geological information available about the fault systems. The criterion adopted to define the predominant style-of-faulting is that of Sadigh et al. (1997), i.e. rake angles between 45° and 135° identify reverse faults while between −45° and −135° identify normal faults, otherwise the mechanism is strike-slip. In some areas, labelled as "undetermined", the data were not sufficient to define a predominant style-of-faulting.

The predictive relations were scaled according to the style-of-faulting only for the larger magnitudes ($M \geq 6$, see Figure 3) because the stronger earthquakes are usually consistent with the predominant style-of-faulting, while smaller earthquakes can be generated by minor faults with different kinematics.

## Attenuation relations from the regional seismicity

In addition to the relations derived from strong-motion databases, in this study we have also used empirical predictive relationships derived from regional weak- and strong-motion data. The background seismicity (largely, weak-motion data) has been used to parameterise the regional attenuation functions as well as some empirical functions of ground-motion duration by Malagnini et al. (2000, 2002) and Morasca et al. (2002). With the aid of the larger events, also the source scaling is quantified for the region. The random vibration theory (RVT, Cartwright and Longuet-Higgins, 1956; Boore, 1983) is then used to predict the absolute levels of ground shaking in terms of peak ground-motion (velocity, acceleration) and spectral accelerations as a function of distance and magnitude.

In Figure 4 are compared the *PHA* predictive relations derived from the scaling laws by Morasca et al. (2002, in the following REG 1) for the Western Alps, Malagnini et al. (2002, in the following REG 2) for the Eastern Alps, and Malagnini and Herrman (2000, in the following REG 3) for the Northern and Central Apennines (all curves are computed for $M_W$ 6.0). According to this figure, Northern and Central Apennines are characterized by a faster decay of ground-motion amplitude compared to the other regions and in particular to Friuli, which is the less attenuative region.

The predictive relationships in Malagnini et al. (2002) were calibrated as follows: first of all, they modelled the empirical regional attenuation using a simple

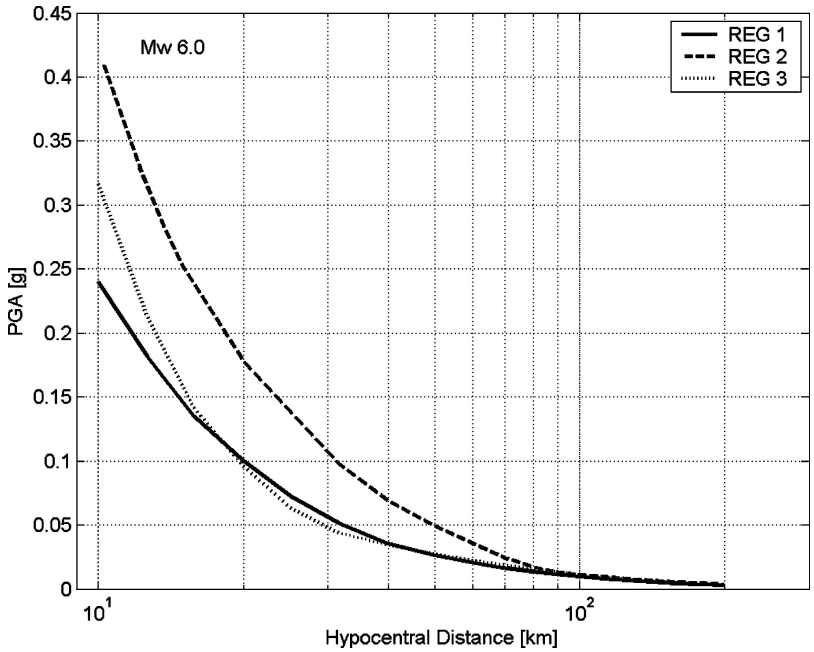


*Figure 4*. Comparison between REG 1, REG 2 and REG 3 for $M_W$ 6.0.

functional form; second, by modelling the behaviour of the small earthquakes at high frequency, they quantified the parameter $\kappa_0$ (corner frequencies of these small earthquakes are supposed to be larger than the highest frequency available); third, the stress parameter $\Delta\sigma$ is calibrated by fitting the spectral amplitudes at high frequency of the largest events in the data set. In the Eastern Alps, an increase of the stress parameter with increasing magnitude was observed by Malagnini et al. (2004). For the Apennines, since the empirical spectra of the small events were too noisy, Malagnini et al. (2000) avoided the calibration of $\kappa_0$, and fixed the stress parameter to 20 MPa, taken from Castro et al. (2001). A zero value for $\kappa_0$ was used to fit the high-frequency spectral amplitudes of the largest event (the Colfiorito mainshock). Malagnini and Herrmann (2000) were able to calibrate the regional parameter $\kappa_0 = 0.04$ sec in the Umbria-Marche region (Central Italy). Since there were only small earthquakes in their dataset, no calibration of $\Delta\sigma = \Delta\sigma(M_W)$ was possible. Hence, in order to produce estimates of the ground shaking at, say, $M_W$ 6.0, the appropriate parameters for the predictive relationships in the Apennines are $\kappa_0 = 0.00$ sec, and $\Delta\sigma = 20$ MPa.

In this study the use of the empirical predictive relationships described above became possible only after a number of operations had been carried out, namely: $M_W$ was computed for all the earthquakes in the catalogue; depth was introduced to convert hypocentral to epicentral distance; different assumptions were adopted to guide the application of the relations outside the regions for which were derived; random variability was quantified; the extrapolation of the relations to the prediction of strong ground-motion was tested with particular regard to large events. In the following, each of these topics will be discussed in detail, except for the magnitude issue, illustrated elsewhere (see Gruppo di Lavoro MPS, 2004).

*Distance conversion*

The regional attenuation relations are defined for hypocentral distances ranging between 10 and 200 km. The conversion to epicentral distances required by SEISRISKIII is relatively easy, provided that the appropriate focal depths are used. We considered two different depth distributions: in one case (Akinci et al., 2004) a uniform focal depth of 10 km was assumed in all non-volcanic areas, which represents the median of the depth distribution of the data used to derive the scaling laws, and 4 km in all volcanic areas. The alternative assumption (Gruppo di Lavoro MPS, 2004), allows the source zones to have different depths based on the modal value of the instrumental focal depths reported in the catalogue. The two models are summarised in Table 3.

*Table 3.* Application of the regional attenuation relations in the seismic source zones and corresponding focal depths, according to model A and model B

| Source Zone | MODEL A | | MODEL B | |
|---|---|---|---|---|
| | Attenuation | Depth [km] | Attenuation | Depth [km] |
| 901 | REG 1 | 10 | REG 1 | 8 |
| 902 | REG 1 | 10 | REG 1 | 10 |
| 903 | REG 1 | 10 | REG 1 | 9 |
| 904 | REG 2 | 10 | REG 2 | 7 |
| 905 | REG 2 | 10 | REG 2 | 8 |
| 906 | REG 2 | 10 | REG 2 | 8 |
| 907 | REG 1 | 10 | REG 1 | 8 |
| 908 | REG 1 | 10 | REG 1 | 10 |
| 909 | REG 1 | 10 | REG 1 | 10 |
| 910 | REG 1 | 10 | REG 1 | 10 |
| 911 | REG 1 | 10 | REG 1 | 8 |
| 912 | REG 2 | 10 | REG 2 | 7 |
| 913 | REG 3 | 10 | REG 3 | 13 |
| 914 | REG 3 | 10 | REG 3 | 13 |
| 915 | REG 3 | 10 | REG 3 | 8 |
| 916 | REG 3 | 10 | REG 3 | 6 |
| 917 | REG 2 | 10 | REG 2 | 7 |
| 918 | REG 3 | 10 | REG 3 | 13 |
| 919 | REG 3 | 10 | REG 3 | 8 |
| 920 | REG 3 | 10 | REG 3 | 6 |
| 921 | REG 4 | 4 | REG 4 | 4 |
| 922 | REG 4 | 4 | REG 4 | 4 |
| 923 | REG 3 | 10 | REG 3 | 9 |
| 924 | REG 2 | 10 | REG 3 | 13 |
| 925 | REG 2 | 10 | REG 3 | 13 |
| 926 | REG 2 | 10 | REG 3 | 13 |
| 927 | REG 1 | 10 | REG 3 | 10 |
| 928 | REG 4 | 4 | REG 4 | 3 |
| 929 | REG 1 | 10 | REG 1 | 10 |
| 930 | REG 1 | 10 | REG 1 | 10 |
| 931 | REG 2 | 10 | REG 3 | 10 |
| 932 | REG 3 | 10 | REG 3 | 13 |
| 933 | REG 3 | 10 | REG 3 | 10 |
| 934 | REG 3 | 10 | REG 3 | 10 |
| 935 | REG 2 | 10 | REG 2 | 13 |
| 936 | REG 4 | 4 | REG 4 | 3 |

Some problems at short distance may arise when using the second assumption: if the focal depth is less than 10 km, the converted epicentral distance will be greater than 1 km. For instance, if the depth is 6 km, the predicted accelerations will be defined only for epicentral distances larger than 8 km, while between 1 and 8 km the acceleration will not be defined. For this reason, we chose to fix the *PHA* value at 1 km epicentral distance equal to the value given by ASB96 (corrected for epicentral distance) for the corresponding $M_S$. We have also assumed that acceleration decays linearly from this value to the closest distance for which the regional relations are defined. The preference given to ASB96 depends on the fact that at close distances it is better constrained by data compared to SP96.

To test how the distance conversion can affect the hazard mapping, we used CRISIS99 (Ordaz et al., 1991), a computer code in which source zone can be located on the surface (as in SEISRISK III) or at depth. For this test, we have selected the source zone 919 located in the Central Apennines and assumed a depth of 10 km (see Figure 5 and Table 3). Using REG 3 (Malagnini et al., 2000) we computed hazard in two ways (Figure 6): in one case (left) the seismic source zone is located on the surface (0 km depth) and depth is used to convert the hypocentral distance of REG 3 to epicentral distance, as done using SEISRISK III. In the other case (right) the seismic source zone is at 10 km depth, and REG 3 is used in its original form as a function of hypocentral distance. The effect of the distance conversion is a slight underestimation of peak acceleration within the source zone, while at large distance no differences can be spotted. Therefore, it can be assumed that correcting the distances in the attenuation tables is equivalent to locating the source zones at depth since the differences are almost negligible.

*Applicability to other regions*

Regional attenuation relations were originally derived only for some regions of Italy, but were assumed to be applicable to other regions showing similar crustal propagation characteristics (Akinci et al., 2004). To do so, two alternative models have been proposed (see Table 3). In the one proposed by Akinci et al. (2004) the empirical predictive relationships derived for the Western Alps by Morasca et al. (2002) can be used also in the Central Alps, in the Southern Apennines and in the Calabrian Arc (zones 929 and 930 in Figure 5). The only studies on attenuation currently available in these areas are those by Eva et al. (1991) on the Western Alps, and by Castro et al. (1999). Eva et al. (1991) found strong lateral variation in attenuation across the Western Alps related to the complex tectonic setting of the area (Morasca et al., 2002). Castro et al. (1999) used a very limited amount of data to infer the S-wave attenuation in NW Italy and found high attenuation up

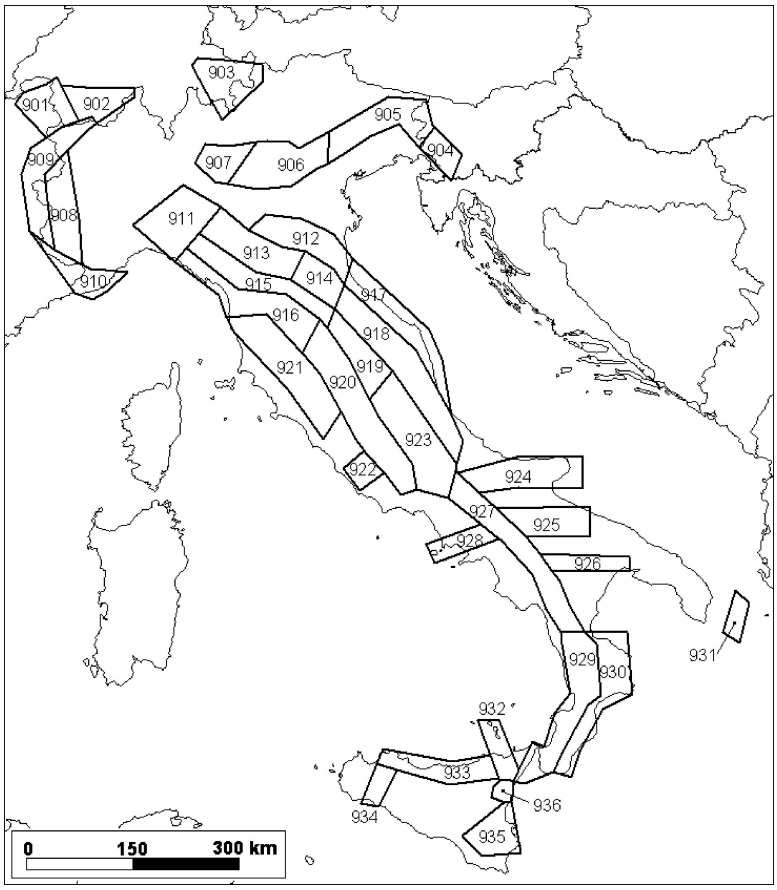


*Figure 5*. Seismic source zones for the 2004 reference seismic hazard map of Italy (from Gruppo di Lavoro MPS, 2004).

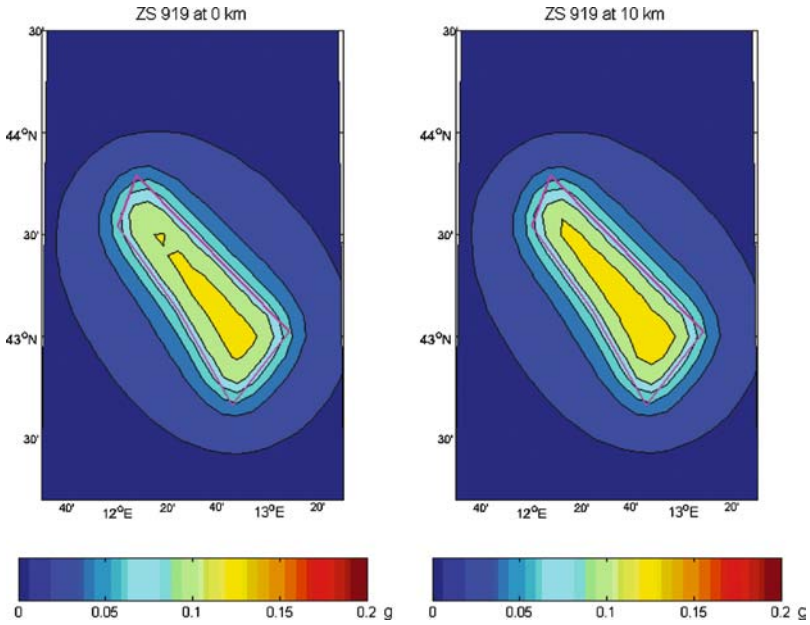


*Figure 6*. Seismic hazard maps for source zone 919 showing the effect of converting hypocentral distance to epicentral distance (*left*) instead of locating the source zone in depth (*right*).

to 10 Hz. Unfortunately, no studies are available for Southern Italy due to the lack of data.

According to Akinci et al. (2004) the attenuation relation derived for Friuli by Malagnini et al. (2002) is applicable to the Eastern Alps, to the Adriatic foreland and to Eastern Sicily. Similar results by Castro et al. (1999) confirm this indication. In fact these authors noted that the regions of Friuli and Marche where seismicity is the result of a compressive tectonic regime, show similar S-wave attenuation, that is less attenuation than in the Central Apennines for all frequencies, while at the larger frequencies attenuation is higher than the average for all Italy. They also found that Eastern Sicily exhibits very little attenuation, being an almost undeformed carbonate platform. Finally, the attenuation by Malagnini and Herrman (2000) derived for the Northern and Central Apennines is applied also in Northern and Western Sicily.

In all the volcanic areas the regional attenuation relation derived by De Natale et al. (1988) from weak-motion data recorded at the Campi Flegrei (Naples) volcanic field was used; this is in reality a scaling relationship of $a_{\max}$ and $v_{\max}$ with respect to seismic moment, containing a simple geometrical attenuation term. These features are apt to match the very fast amplitude decay from shallow earthquake sources typical of volcanic regions.

The model described above, used together with the uniform depth distribution (Akinci et al., 2004) presented in the previous section, will be indicated in the following as model A.

The second model, proposed by Gruppo di Lavoro MPS (2004), introduces some modifications only in Southern Italy where the information is less abundant compared to other regions. It is assumed that the Apulian plateau (seismic source zones 924, 925 and 926 in Figure 5), belonging to the Adriatic foreland, and the Southern Apennines have the same attenuation characteristics as the Northern and Central Apennines. This second model, together with the non-uniform depth distribution, will be referred to as model B.

*Random variability*

A measure of the random variability is provided in ground-motion predictive relations through the standard deviation ($\sigma_{\log Y}$) and it is easily incorporated in seismic hazard analysis (Bender, 1984). Not so for the empirical predictive relationships derived from scaling laws. The issue of estimating the standard deviation associated with a stochastically-derived ground-motion prediction is complex; Toro et al. (1997) deal with this topic in a thorough and rigorous manner. The values provided for the standard deviation of the peak acceleration estimates are respectively 0.20, 0.22 and 0.18 for the relations by Morasca et al. (2002), Malagnini et al. (2002) and Malagnini and Herrman (2000). These authors obtained the uncertainties associated with the ground-motion at large magnitudes by using regressions of a mix of weak- and strong-motion data. The regressions on the observed spectra were carried out as a function of frequency, regardless of the magnitude of the specific events used. Ground-motion predictions have been subsequently obtained through RVT, and the variances associated to the peak values at a given magnitude, had to be based on the predominant frequency of radiation at that specific earthquake's size. Since most of the interest would be on larger events, the variance corresponding to the predominant frequency of zero-crossing for these events was chosen. In other words, the energy radiation of an event, given its magnitude, is basically centred at its corner frequency (the predominant frequency in the velocity spectrum); consequently, the predominant frequency of zero-crossing for the de-trended seismograms is to be chosen accordingly. Regression residuals of the spectral ordinates at that specific frequency (we chose 1.0 Hz for this study) were then used for the computation of the data standard error. Obviously, this process contains unavoidable elements of arbitrariness.

No measure of dispersion was available for the De Natale et al. (1988) relation because it has been derived for a different purpose, i.e. to show how well an $\omega$-square model could explain the dependence of $v_{\max}$ and $a_{\max}$ on $M_0$.

The standard deviation values of the regional relations cannot be directly compared with those provided for ASB96 or SP96; therefore, to ensure that these values are compatible and can be used in seismic hazard analysis we performed an empirical test. We collected the *PHA* values corresponding to the larger horizontal component of a number of Italian records (rock or very stiff soils only) from earthquakes with magnitudes ranging from 4 to 7. These data were divided into magnitude ranges with a step of 0.5 and into regions according to the model A. For each group of data we computed the predicted *PHA* using ASB96 (with $M_S$), SP96 (with $M_L$ and $M_S$) and the regional relation (with $M_W$) and evaluated the standard deviation of the residuals. The results are summarized in Table 4 while Figure 7 shows the residuals computed using *PHA*

*Table 4.* Standard deviation of the residuals between observed and predicted peak horizontal accelerations, computed for different magnitude classes using: (i) the regional attenuation relations according to model A; (ii) ASB96; (iii) SP96. The standard deviation has been computed as $\sigma = [\sum_{i=1}^{n} (\text{obs} - \text{pred}^2/(n-1)]^{\frac{1}{2}}$. $M = M_W$ for the regional empirical predictive relationships; $M = M_S$ for ASB96; $M = M_L$ for $M < 5.5$ and $M_S$ otherwise for SP96

| MODEL A | Western Alps Southern Apennines Calabrian Arc | | | Eastern Alps Apulian Plateau Eastern Sicily | | | Central Apennines Northern Sicily | | |
|---|---|---|---|---|---|---|---|---|---|
| *M* | REG 1 | ASB96 | SP96 | REG 2 | ASB96 | SP96 | REG 3 | ASB96 | SP96 |
| 4.0 | 0.0639 | 0.0607 | 0.0520 | 0.0265 | 0.0116 | 0.0204 | – | – | – |
| 4.5 | 0.0583 | 0.0490 | 0.0368 | 0.0676 | 0.0948 | 0.0686 | 0.0327 | 0.1438 | 0.0473 |
| 5.0 | 0.0142 | 0.0152 | 0.0365 | 0.0440 | 0.0487 | 0.0677 | 0.0461 | 0.0752 | 0.0493 |
| 5.5 | 0.0566 | 0.0714 | 0.0587 | 0.0308 | 0.0302 | 0.0268 | 0.0607 | 0.0512 | 0.0490 |
| 6.0 | 0.0713 | 0.0771 | 0.1105 | 0.0633 | 0.0331 | 0.0208 | 0.0711 | 0.0813 | 0.0554 |
| 6.5 | – | – | – | 0.0543 | 0.1105 | 0.0936 | 0.0555 | 0.0548 | 0.0419 |
| 7.0 | 0.0964 | 0.1215 | 0.1048 | 0.1282 | 0.1055 | 0.1415 | – | 0.0134 | 0.0321 |
| Average | 0.0601 | 0.0658 | 0.0666 | 0.0592 | 0.0621 | 0.0628 | 0.0532 | 0.0700 | 0.0458 |

values recorded in the Eastern Alps, Apulian plateau and Eastern Sicily (left) and in Central Apennines and northern Sicily (right), for $M$ ranging between 4.75 and 6.75 (grouped in four $M$ classes: 5.0, 5.5, 6.0 and 6.5), and *PHA* predicted by REG 2 and 3 respectively (filled triangles), by ASB96 (open circles) and SP96 (plus symbol). The comparison indicates that on average the prediction of the regional attenuation relations is comparable to ASB96 predictions. It also shows that the associated values of standard deviation are reliable and can be used in seismic hazard analysis. Unfortunately, the SEISRISKIII code can apply only a single value of standard deviation, so it was agreed to use the value $\sigma_{\log Y} = 0.20$ for all the regional relations, included the one for volcanic areas. This value is in good accord with the standard deviation of SP96 relation, equal to 0.19. This relatively small value is in part the result of selective treatment of the available data set.

### *Applicability of the regional seismicity-based attenuation relations (empirical predictive relationships) to strong-motion prediction*

The applicability of the regional relations has been empirically verified comparing the prediction with strong-motion data recorded at hard ground sites in Italy. The comparisons can be considered to provide an independent validation of the empirical predictive relationships, because these were derived using weak-motion data, with the only exception of Friuli (NE Italy) region. Actually, in Friuli both the available accelerograph recordings and the weak-motion data were included in the derivation of the regional scaling relations. As an example, in Figure 8 are compared the strong-motion data recorded during the 1980 Irpinia mainshock ($M_W$ 6.9) with the corresponding attenuation curves provided by the two regional models illustrated.

As magnitude increases, important changes occur in the observed attenuation characteristics, which are accounted for in the regional attenuation relations (see Figure 9). In this study, it was necessary to compute peak accelerations also for magnitudes higher than those of the strongest events included in the databases used to derive the relations, in particular: above $M_W$ 6.5 in the Eastern Alps; above $M_W$ 6.0 in the Central Apennines; above $M_W$ 5.4 in the Western Alps (Gruppo di Lavoro MPS, 2004). As shown in Figure 9, the decay with distance of the peak acceleration is steeper for smaller magnitudes, and gets less and less steep as the magnitude increases. This is because the predictive relationships for the peak ground-motion are calculated using RVT, through a specific spectral model that radiates energy mostly around the corner frequency. The latter varies strongly with magnitude, and so does the crustal parameter $Q = Q(f)$. It is thus clear that, at a specific distance from the source, the peak ground-motion is carried by different frequencies at different magnitudes, and so its distance decay rate must as well vary as a function of magnitude.

To validate the extrapolation we compared the prediction with strong-motion data recorded at hard

ground sites in regions with similar crustal attenuation characteristics. In particular we compared the predicted ground-motion obtained with REG 2 with records of the 1979 Montenegro ($M_W$ 6.9) earthquake, because it was generated in a similar compressive tectonic regime (Figure 10, left). Based on analogous considerations we compared the prediction obtained with REG 3 with strong-motion records from a number of Greek normal fault earthquakes of $M_W$ 6.5 (Figure 10, right). It must be noted though, that strong-motion records from Greece and Montenegro are not necessarily recorded in free-field conditions.

## Volcanic areas

Predicting earthquake ground-motion in volcanic areas or in neighbouring regions raises the problem of modelling the propagation of seismic waves through volcanic rocks. It is known that in volcanic areas the shallow earthquake sources (focal depth typically less than 5 km) together with the presence of highly fractured rocks possibly filled by gas or viscous fluids, tend to lower the capability of transmitting high-frequency ground-motions (Minakami, 1974; Chouet et al., 1987; Patanè et al., 1994; Nishimura et al., 1995; Munson

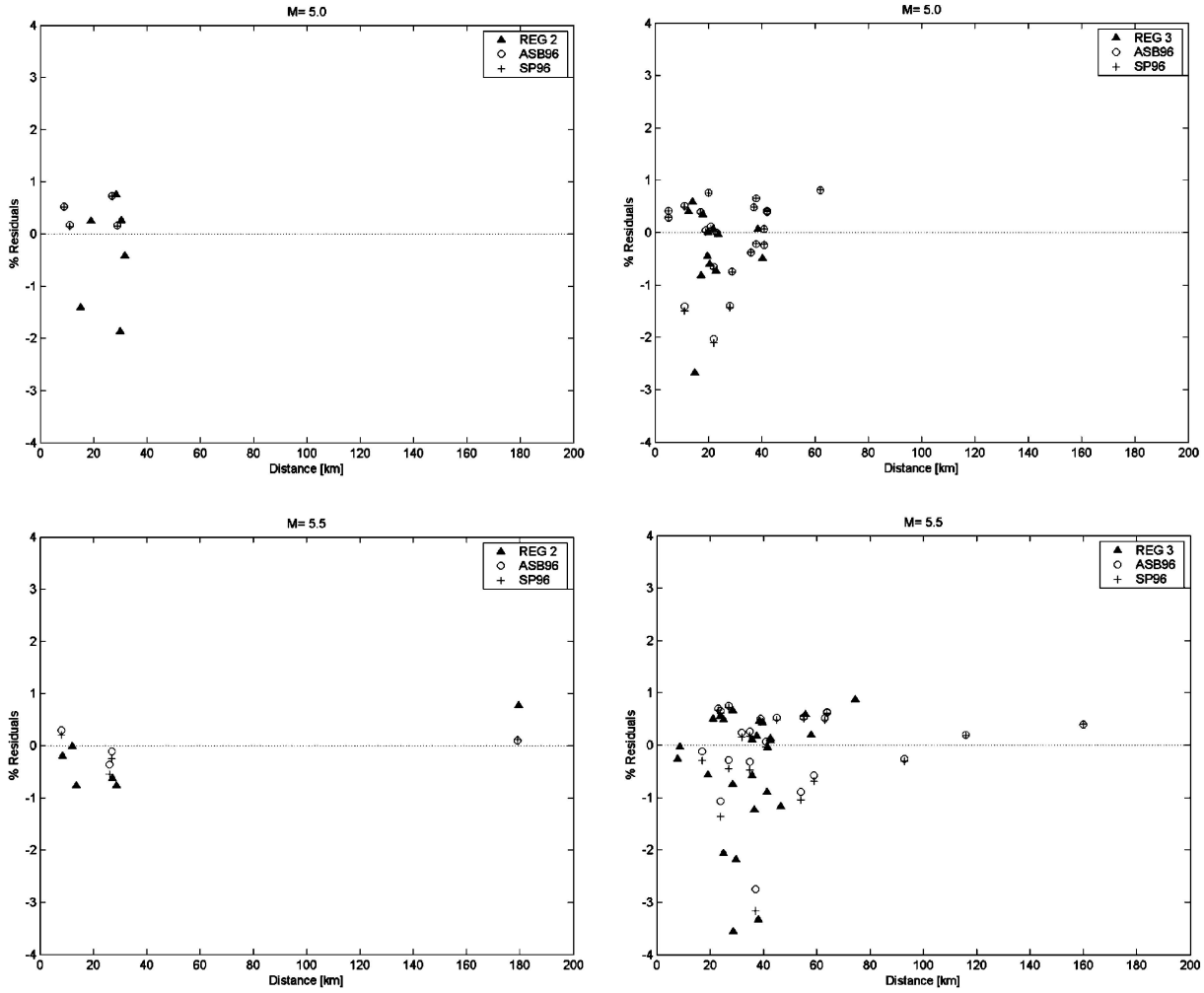


*Figure 7.* Residuals between observed and predicted peaks of acceleration, computed using the regional empirical predictive relationships (*filled triangles*), ASB96 (*open circles*) and SP96 (*plus symbol*), for different magnitude classes ($M$ = 5.0, 5.5, 6.0 and 6.5). The figures on the left show the residuals computed using records from the Eastern Alps, Apulian plateau and Eastern Sicily and REG 2. The figures on the right are computed for the Central Apennines and Northern Sicily and REG 3 ($M = M_W$ for REG 3; $M = M_S$ for ASB96; for SP96 $M = M_L$ when $M < 5.5$, and $M_S$ otherwise).

(*Continued on next page*)

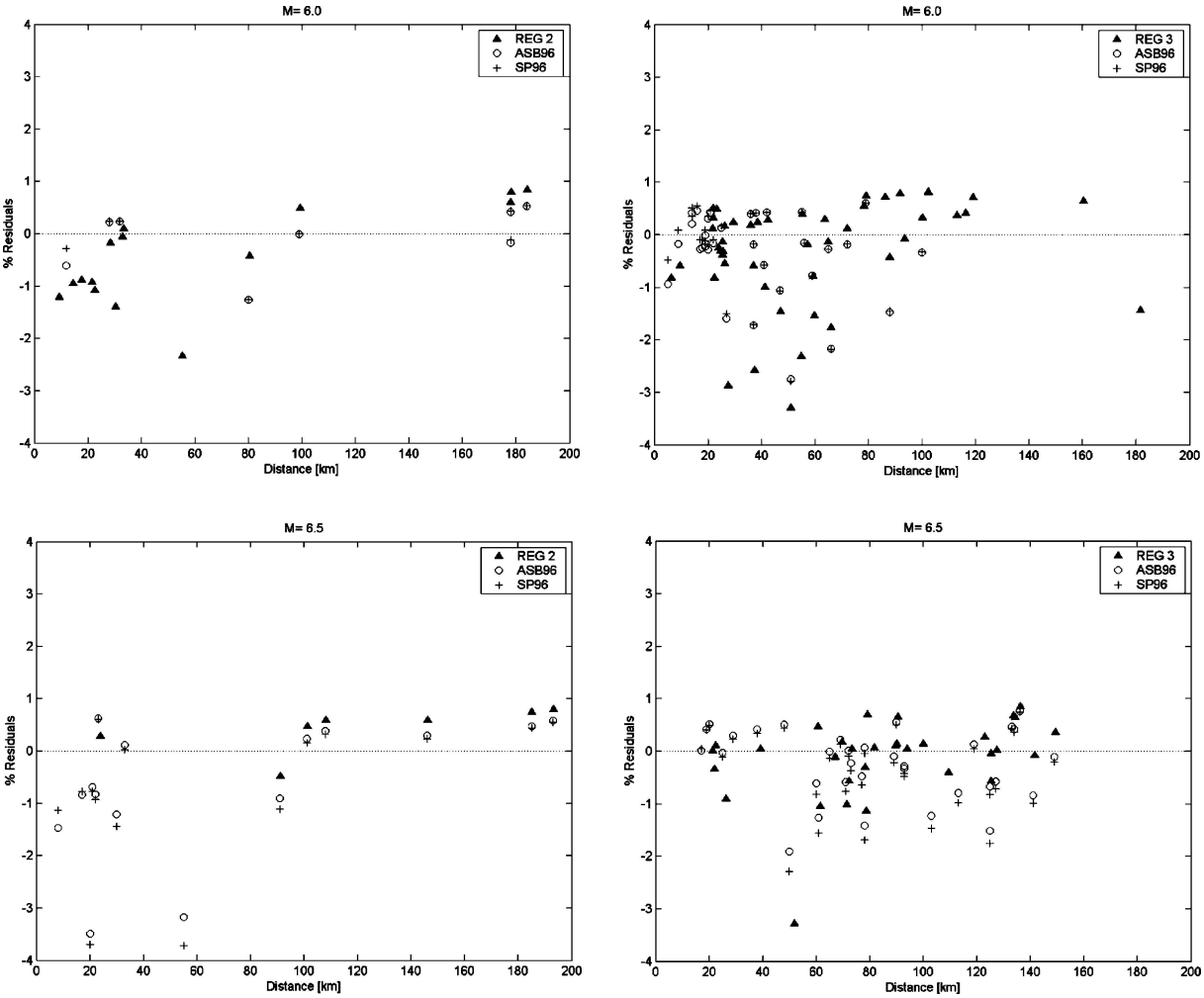


*Figure 7.* (*Continued*)

and Thurber, 1997). Evidence of strong attenuation in the upper layers of volcanic structures is provided also by the observed damage patterns of moderate or low magnitude events ($M < 5$), usually showing heavy damage in the small epicentral area and a fast decay with distance, so that hardly any effects are observed few km away. For example, the $M_W$ 4.9, 1971 Tuscania earthquake occurred in Southern Tuscany produced local intensities as high as 8/9 MCS (Monachesi and Stucchi, 1997). Although there is no theoretical correlation available among MCS intensities and those of other scales, it is generally accepted that MCS intensities indicate damage level equal to or slightly higher than the one described by the same values in MSK or EMS98 scales, the difference not exceeding the intrinsic uncertainty of any intensity estimate.

Usually, seismic hazard in active volcanic regions around the world is computed without using specific predictive relations or adjustments accounting for the peculiar propagation characteristics of these areas (Dimaté et al., 1999; Zhang et al., 1999; Grünthal et al., 1999; Midzi et al., 1999; Kijko and Öncel, 2000). Some exceptions are the seismic hazard maps of Hawaii and of Italy. In fact, the seismic hazard map of Hawaii proposed in 1998 by Klein et al. (2001) and its recent update (2002) have been produced introducing in a logic tree four different predictive relations, among which the Munson and Thurber (1997) relation derived from Hawaiian earthquakes. All the relations were referred to firm rock condition corresponding to sites on lava flows, and received equal weight. In previous seismic hazard maps of Italy (Slejko et al., 1998, 1999;

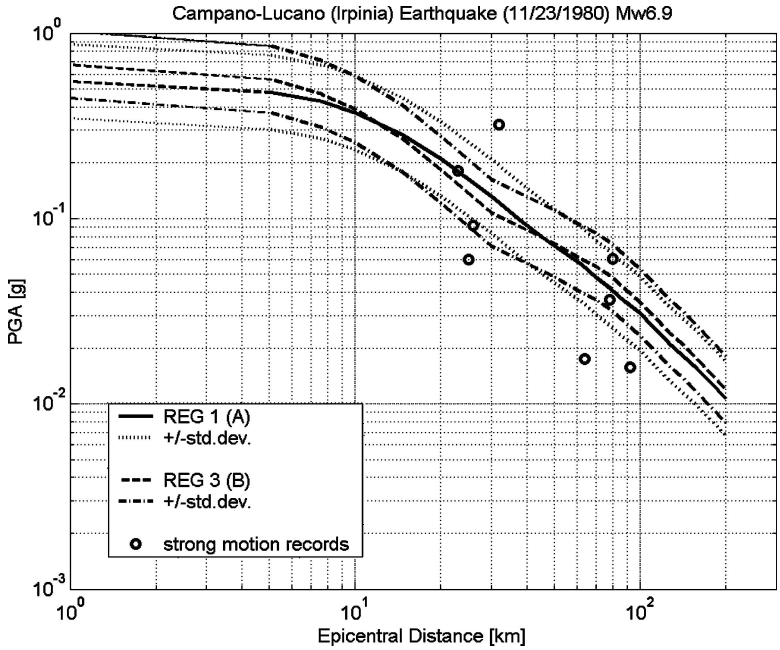


*Figure 8.* Comparison between attenuation curves and strong-motion records of the 1980 Irpinia earthquake ($M_W$ 6.9). Model A (*solid and dotted lines*) uses REG 1 and a depth of 10 km; model B (*dashed and dash-dotted lines*) uses REG 3 and 10 km depth.

Albarello et al., 2000) attenuation in the main volcanic areas has been accounted for, in a rough way, by simply reducing the predicted ground-motion by a fraction of the standard deviation. In the Etna source zone, Albarello et al. (2000) used a specific attenuation derived from macroseismic data.

In the present project hazard was computed in four volcanic regions, i.e. the geothermal area along the Tirrenian coast of Tuscany related to an astenospehric upwelling (source zone 921); the volcanic structures belonging to the Quaternary Roman Magmatic province (including the Alban Hills volcano near Rome – source zone 922); the Campanian volcanic area, near Naples, including Mt Vesuvius, Campi Flegrei volcanic field and Ischia (source zone 928), and the Mt Etna volcano (source zone 936). As in the other source zones, ASB96 and SP96 predictive relations adjusted for style-of-faulting were employed in the volcanic areas mentioned above. In the regional branches of the logic tree, we used the scaling relation originally derived by De Natale et al. (1988) for the Campi Flegrei (Naples) area, assuming a depth of 4 km for all volcanic source zones in model A, while model B allowed the Etna and Alban Hills area to have a slightly shallower depth.

The De Natale et al. (1988) relation was computed from a set of high quality digital records of 40 events occurred during the ground uplift episode that took place in the Campi Flegrei area between 1982 and 1984. The magnitude of the events ranges between $0.7M_L$ and $3.2M_L$ and the distance is generally short (3 to 6 km). The attenuation parameters computed include both geometric spreading $(1/r)$ and a $\kappa$ value of $0.015 \pm 0.020$, corresponding to an equivalent $Q$ of about 250 at an average distance of 5 km (De Natale et al., 1988).

Two different values of the stress parameter were alternatively used to predict *PHA*: a value of 50 bar was used for the larger source zones (e.g. the coastal area of Tuscany and the Neapolitan volcanic system) because they encompass a number of different earthquakes some of which may occur at greater depth, while a stress parameter of 30 bar was used in the other two volcanic areas (Alban Hills and Mt Etna) to account for smaller and shallower sources (Figure 11).

Predictive relations in terms of *PHA* were calculated by means of RVT as described in the previous section, for magnitude ranging between 3.0 and 6.5 and hypocentral distance not greater than 20 km. Unfortunately, these curves could not be checked for consistency with observed strong-motion data because records available from the published databases are very scanty. Nonetheless, the use of observed macroseismic intensities, as reported in the database DOM4.1 (Monachesi and Stucchi, 1997), allowed an indirect validation of the regional relations. We have compared

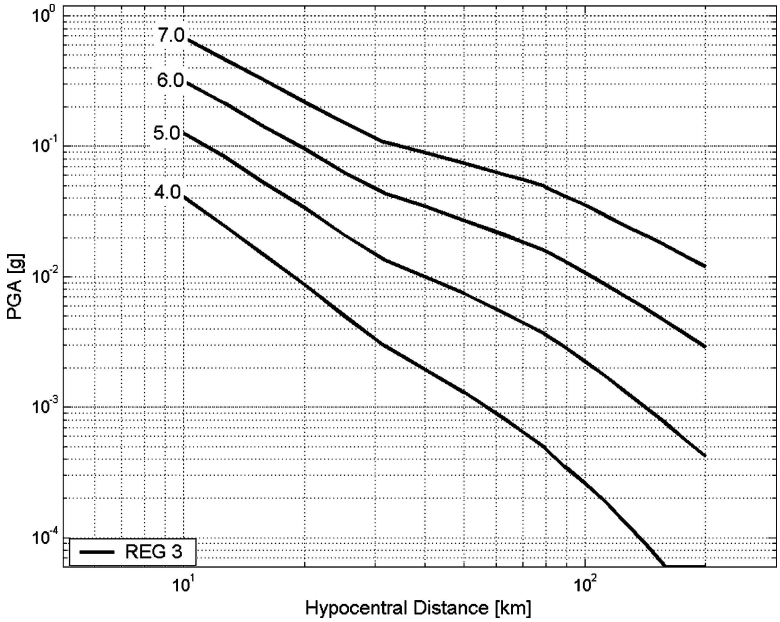


*Figure 9.* Attenuation curves (REG 3) for $M_W$ 4.0, $M_W$ 5.0, $M_W$ 6.0 and $M_W$ 7.0.

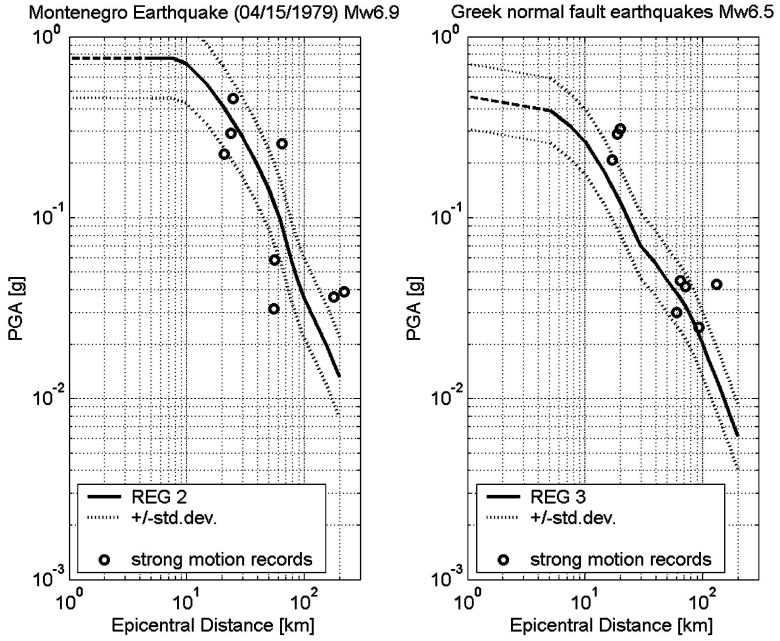


*Figure 10. Left*: Comparison between REG 2 attenuation curves and strong-motion records of the 1979 Montenegro earthquake ($M_W$ 6.9), assuming a depth of 10 km; *Right:* Comparison between REG 3 attenuation curves and strong-motion records of several Greek normal fault earthquakes ($M_W$ 6.5), assuming a depth of 10 km.

the observed intensities ($I_{MCS}$) of two earthquakes occurred in volcanic areas (1952 Etna and 1971 Tuscania earthquake) with the predicted intensities obtained converting the peaks of velocity computed with REG 4 and with SP96 (Figure 12). We used the conversion relation:

$$I_{MCS} = 1.719 \log(v_{\max}) + 5.1491 \quad \sigma = \pm 0.646 \quad (6)$$

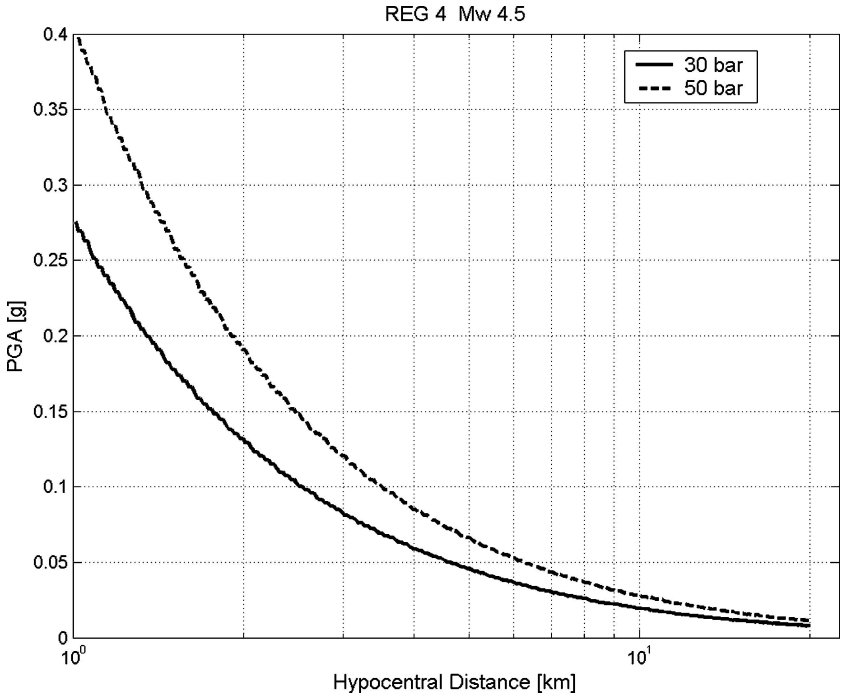


*Figure 11.* Regional attenuation for volcanic areas (REG 4) computed for $M_W$ 4.0 using different stress parameters: *solid line* for 30 bar, *dashed line* for 50 bar.

valid from $I_{MCS}$ 4 to 9 (Faccioli et al., 2004). This relation was derived from a data set including 81 observed intensities from 23 earthquakes occurred in Italy, Greece (three earthquakes, among which Athens 1999) and Turkey (Izmit, 1999). The MSK intensities from the Turkish earthquake data were assumed to be equal to MCS intensities.

The faster decay of REG 4 relation is much more consistent with the observed intensities compared to the prediction of a standard ground-motion attenuation relation such as SP96.

## Influence of the attenuation options and weighting scheme

To illustrate the consequence of treatment on final results in Figure 13 (from Gruppo di Lavoro MPS, 2004) are shown four hazard maps of Italy obtained using different attenuation relations. Each of these maps represents mean acceleration values from the weighting scheme of the logic tree. The maps obtained from ASB96 and SP96 (respectively Figure 13a and b) are almost similar, with ASB96 providing higher (about 0.025 g) ground-motion levels in all the regions. The maps obtained with the regional attenuations using model A (Figure 13c) and model B (Figure 13d) differ in several areas because: 1) model B uses different focal depths compared to model A (e.g. NE Italy, Central Italy, Eastern Sicily, see also Table 3); 2) model B uses a different attenuation relation compared to model A (e.g. Apulian plateau in Southern Italy, corresponding to source zones 924, 925 and 926).

For the purpose of computing the reference seismic hazard map of Italy (available at the URL http://www.zonesismiche.mi.ingv.it), it was decided to attribute equal weight to the three attenuation relations that is 0.33 to SP96, 0.33 to ASB96 and 0.34 to the regional relations. The latter is to be divided equally between model A and model B (receiving 0.17 each). Since SEISRISK III is not designed to compute hazard through a formal logic tree approach, 16 independent hazard maps were computed and combined according to the logic tree, in a post-processing stage. In this framework the only way to assign a higher weight to REG 4 compared to SP96 and ASB96, would be to extract the areas from the surrounding regions and treat them separately. Based on the evidences shown in Figure 12, our choice can be interpreted as a rather conservative solution.

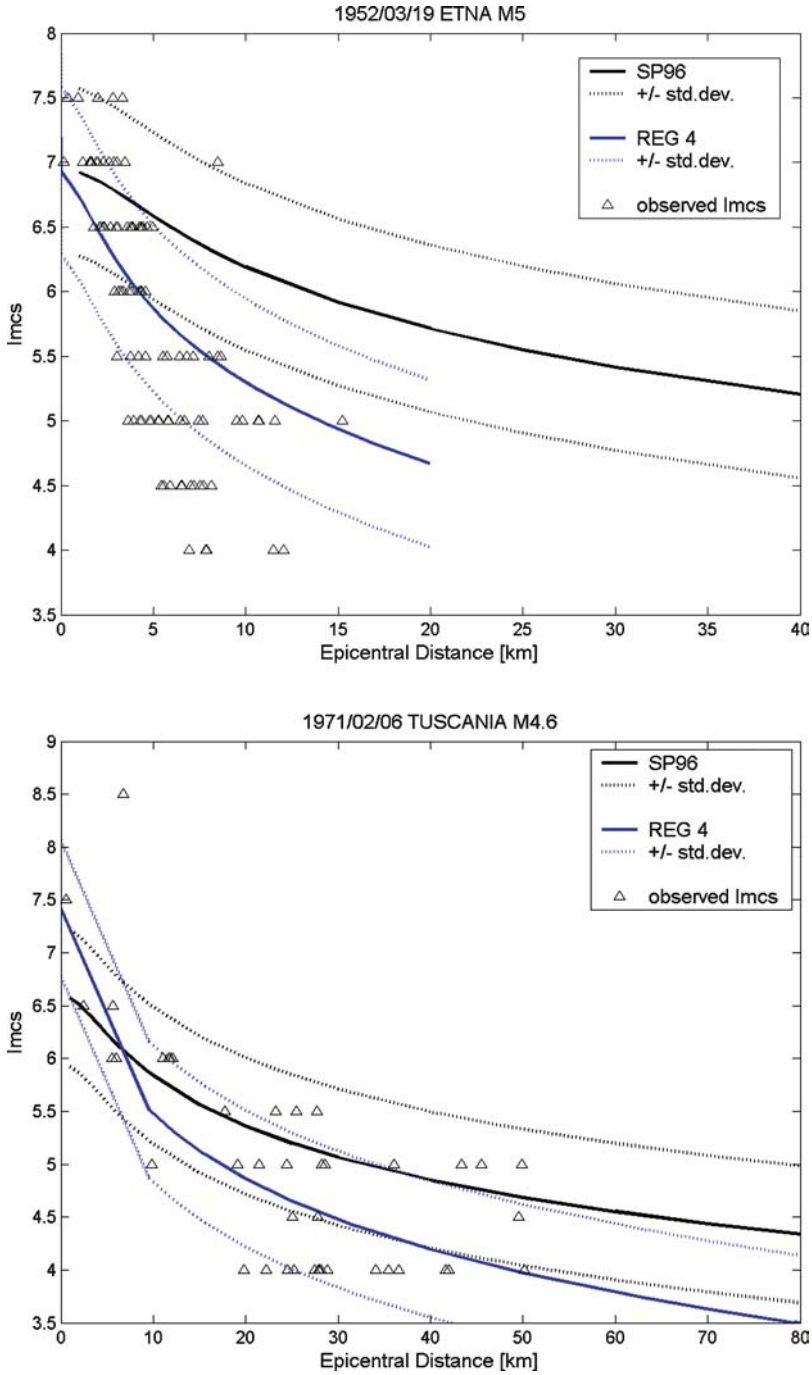


*Figure 12*. Comparison between observed intensities (MCS scale, *open triangles*) and intensities (converted from peak of velocity) predicted using SP96 (*in black*) and REG 4 (*in blue*), for two earthquakes: 1952 Etna earthquake (*on top*) and 1971 Tuscania (Southern Tuscany) earthquake (*at the bottom*).

## Conclusions

We illustrated in the previous sections mainly how strong ground-motion attenuation and related issues were dealt with in a research project leading in 2004 to a new seismic hazard map for Italy. By way of conclusive comments, we would like to stress in the first place the rigorous effort made to achieve consistency

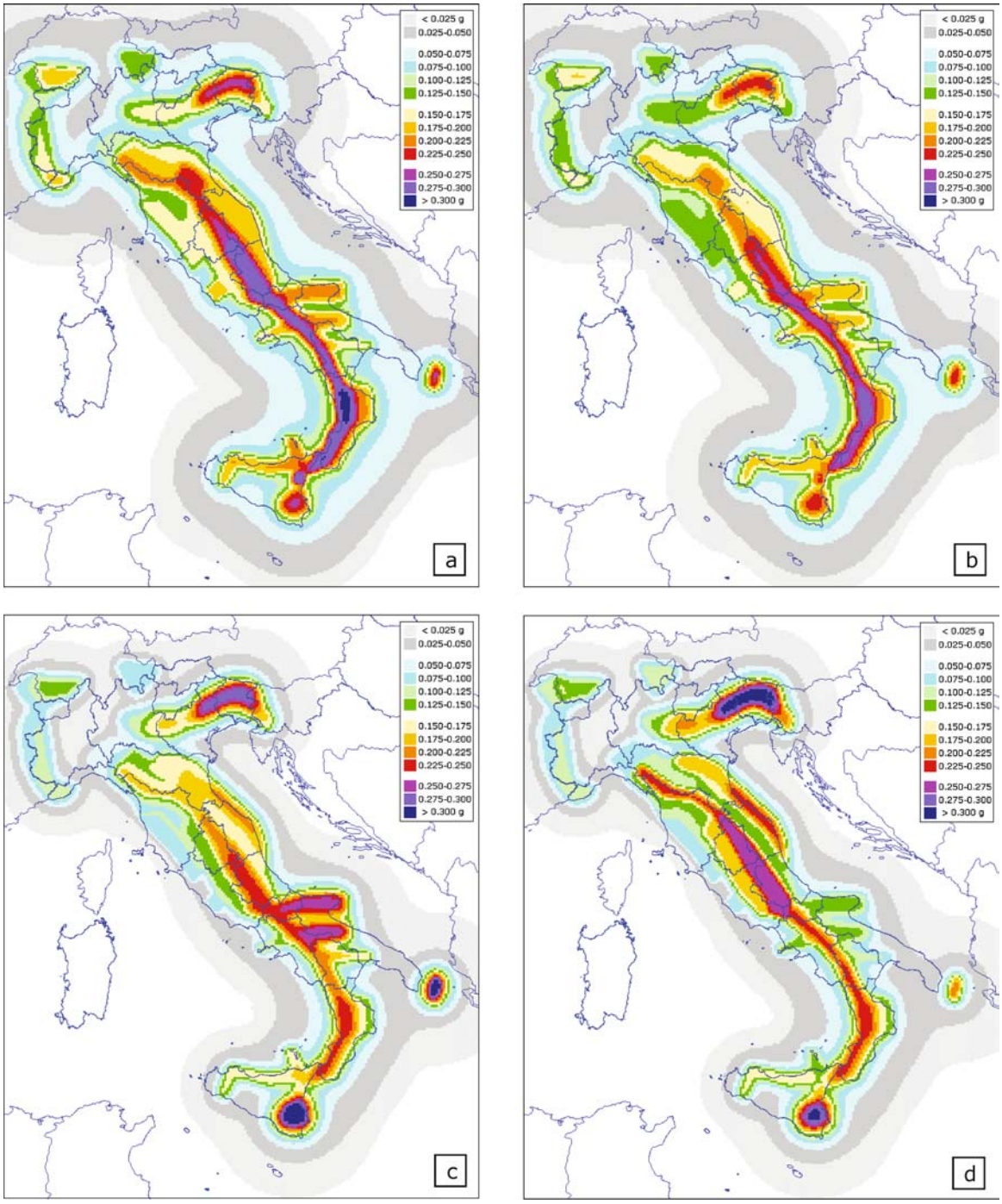


*Figure 13*. Seismic hazard maps of Italy computed using different attenuation relations: (a) ASB96; (b) SP96; (c) regional attenuations according to model A; (d) regional attenuations according to model B (from Gruppo di Lavoro MPS, 2004).

among the main ingredients entering in the overall hazard evaluation picture.

Perhaps the basic block in such effort was the full use made of the available geological and seismological knowledge. Motivated by the application of scaling coefficients and by the need of consistency among different attenuation relations, significant refinements were made to the seismic source zones, such as introducing

the predominant syle-of-faulting and the average depth (Gruppo di Lavoro, 2004).

Other main consistency requirements resulted on one hand, in preparing a new earthquake catalogue for Italy (not described herein) that contains the magnitudes $M_S$, $M_W$, $M_L$ required by the different attenuation relations employed and, on the other hand, in suitably modifying the distance measures used in such relations in order to make them adapted to the single, restrictive measure allowed in the computational tool chosen (the SEISRISK III code). We are not aware of a comparable effort encompassing all these issues together made in any other European country or elsewhere for the purpose of hazard mapping.

In the second place, a feature of this study that may lay some claim in the way of innovation in seismic hazard studies, is the systematic use of "regional" empirical predictive relations for ground-motion attenuation, including those specifically developed for volcanic areas, side by side with well known standard relations. The regional relations were calibrated in most (not all) cases on large datasets of weak-motion records only, but empirical checks with available strong-motion data show that the predictions obtained are in no way inferior to those of strong-motion based attenuation relations, and in some cases are actually better. Salient assets of the regional relations are the magnitude dependence of the shape of the attenuation functions, and the apparent ability of well tested source and spectral radiation models to allow realistic extrapolation from weak- to strong-motion events (although the basic issue of whether the source rupture physics of small and large earthquakes is similar remains in part unclear). The single maps in Figure 13 bring out very clearly the impact of the regional relations for zones of low attenuation (such as NE Italy and SE Sicily), or of higher than normal attenuation (such as the Mt. Etna and the Naples regions).

Regional predictive relations derived from weak-motion data can be obtained even in regions where strong-motion records are not available, as is the case in most of Southern Italy, in the NW Alps and in volcanic regions. Moreover, in these situations, intensity data points (Figure 12) can also be a significant source of information in order to identify (at least qualitatively) the characteristics of attenuation. In our study, macroseismic data were used only in volcanic areas simply because extending the comparison to all regions was beyond the scope and the time constraints of the project.

The use of at least 4 groups of predictive ground-motion relations is the main tool that has allowed to tackle with epistemic uncertainty affecting strong-motion attenuation, in the context of a logic tree approach. The number of branches in such a tree was obviously kept limited by the size of the overall task, i.e. calculating hazard not at a single site but over a grid of nearly 60 000 points covering all Italy.

Finally, it is perhaps apt to remind here that the derivation of new hazard maps was pointed out as an urgent need for many European countries in a recent study (García-Mayordomo et al., 2004). The approach highlighted in our study is believed to be a good starting point specifically as regards an enhanced definition of the source zone characteristics, need of producing earthquake magnitude consistent with those required in attenuation relations, consistency of distance metrics between computational codes and attenuation relations, and exploring the feasibility of regional predictive relations.

## Acknowledgements

The authors are grateful to Julian Bommer and to an anonymous reviewer for their comments and suggestions. Massimiliano Stucchi and Carlo Meletti are acknowledged for their help and support throughout the project.

## References

Akinci, A., Mueller, C., Malagnini, L. and Lombardi, A., 2004, Seismic hazard estimate in the Alps and Apennines (Italy) using smoothed historical seismicity and regionalized predictive ground-motion relationships, *Boll. Geofis. Teor. Appl.* **45**, 285–304.

Albarello, D., Bosi, V., Bramerini, F., Lucantoni, A., Naso, G., Peruzza, L., Rebez, A., Sabetta, F. and Slejko, D., 2000, Carte di pericolosità sismica del territorio nazionale, *Quaderni di Geofisica*, 12, ING, Roma, 7 pp., CD-ROM, 4 annexes (in Italian).

Ambraseys, N.N., 1995, The prediction of earthquake peak ground acceleration in Europe, *Earthquake Eng. Struct. Dyn.* **24**, 467–490.

Ambraseys, N.N. and Bommer, J.J., 1991a, The attenuation of ground accelerations in Europe, *Earthquake Eng. Soil Dyn.* **20**, 1179–1202.

Ambraseys, N.N. and Bommer, J.J., 1991b, Database of European strong ground-motion records, *Eur. Earthquake Eng.* **2**, 18–37.

Ambraseys, N.N., Simpson, K.A. and Bommer, J.J., 1996, The prediction of horizontal response spectra in Europe, *Earthquake Eng. Struct. Dyn.* **25**, 371–400.

Ambraseys, N.N., Smit, P., Douglas, J., Margaris, B., Sigbjornsson, R., Olafsson, S., Suhadolc, P. and Costa, G., 2004, Internet-site for European strong-motion data, *Boll. Geofis. Teor. Appl.* **45**, 113–129, http://www.isesd.cv.ic.ac.uk/.

Bender, B., 1984, Incorporating acceleration variability into seismic hazard analysis, *Bull. Seism. Soc. Am.* **74**, 1451–1462.

Bender, B. and Perkins, D.M., 1987, SEISRISK III – A computer program for seismic hazard estimation, *US Geol. Surv. Bull.* **1772**, 1–20.

Bommer, J.J., Douglas, J. and Strasser, F.O., 2003, Style-of-faulting in ground-motion prediction equations, *Bull. Earthquake Eng.* **1**, 171–203.

Bommer, J.J., Scherbaum, F., Bungum, H., Cotton, F., Sabetta, F. and Abrahamson, N.A., 2005, On the use of logic trees for ground-motion prediction equations in seismic hazard analysis, *Bull. Seism. Soc. Am.* **95**, 377–389.

Boore, D.M., 1983, Stochastic simulation of high-frequency ground motions based on seismological models of the radiated spectra, *Bull. Seism. Soc. Am.* **73**, 1865–1894.

Cartwright, D.E. and Longuet-Higgins, M.S., 1956, The statistical distribution of the maxima of a random function, *Proceedings of the Royal Soceity (London)* Ser. **A237**, 212–232.

Castro, R.R., Mucciarelli, M., Monachesi, G., Pacor, F. and Berardi, R., 1999, A review of nonparametric attenuation functions computed for different regions of Italy, *Ann. Geofis.* **42**, 735–748.

Castro, R.R., Rovelli, A., Cocco, M., Di Bona, M. and Pacor, F., 2001, Stochastic simulation of strong-motion records from the 26 September 1997 ($M_W$ 6) Umbria-Marche (Central Italy) earthquake*, Bull. Seismol. Soc. Am.* **91**, 27–39.

CEN, May 2004, *European Committee for Standardisation. Eurocode 8: Design of Structures for Earthquake Resistance. Part 1: General Rules, Seismic Actions and Rules for Buildings, European Standard EN 1998-1: 2004 (stage 51)*, Brussels, 229 pp.

Chouet, B., Koyanagi, R.Y. and Aki, K., 1987, Origin of volcanic tremor in Hawaii (part II): Theory and discussion. In Decker, R.W., Wright, T.L. and Stauffer, P.H. (eds.), *Volcanism in Hawaii*, US Geological Survey Professional Paper 1350, Vol. II, 1259–1280.

Coppersmith, K.J. and Youngs, R.R., 1986, Capturing uncertainty in probabilistic seismic hazard assessment within intraplate tectonic environments. In *Proceedings of the Third US National Conference on Earthquake Engineering*, **1**, 301–312.

Cornell, C.A., 1968, Engineering seismic risk analysis, *Bull. Seism. Soc. Am.* **58**, 1583–1606.

De Natale, G., Faccioli, E. and Zollo, A., 1988, Scaling of peak ground-motions from digital recordings of small earthquakes at Campi Flegrei, Southern Italy, *Pure Appl. Geophys.* **126**, 37–53.

Dimaté, C., Drake, L., Yepez, H., Ocola, L., Rendon, H., Grünthal, G. and Giardini, D., 1999, Seismic hazard assessment in the Northern Andes (PILOTO Project), *Ann. Geofis.* **42**, 1039–1055.

Eva, C., Cattaneo, M., Augliera, P. and Pasta, M., 1991, Regional coda Q variations in the Western Alps (northern Italy), *Phys. Earth Planet. Inter.* **67**, 76–86.

Faccioli, E., Frassine, L., Finazzi, D., Pessina, V., Cauzzi, C., Lagomarsino, S., Giovinazzi, S., Resemini, S., Curti, E., Podestà, S., and Scuderi, S., 2004, Synthesis of the application to Catania city. Report of EC Project RISK-UE (An advanced approach to earthquake risk scenarios with applications to different European towns), Contract: EVK4-CT-2000-00014. http://www.risk-ue.net.

García-Mayordomo, J., Faccioli, E. and Paolucci, R., 2004, Comparative study of the seismic hazard assessments in European national seismic codes, *Bull. Earthquake Eng.* **2**, 51–73.

Giardini, D., 1999, The global seismic hazard assessment program (GSHAP) – 1992/1999, *Ann. Geofis.* **42**, 957–974.

Grünthal, G. and the GSHAP Region 3 Working Group, 1999, Seismic hazard assessment for Central, North and Northwest Europe: GSHAP Region 3, *Ann. Geofis.* **42**, 999–1011.

Gruppo di Lavoro MPS, 2004, *Redazione della mappa di pericolosità sismica prevista dall'Ordinanza PCM 3274 del 20 marzo 2003. Rapporto Conclusivo per il Dipartimento della Protezione Civile*, INGV, Milano-Roma, April 2004, 65 pp. + 5 annexes (in Italian). http://zonesismiche.mi.ingv.it/documenti/rapporto_conclusivo.pdf.

Jiménez, M.J., Giardini, D., Grünthal, G. and the SESAME Working Group, 2001, Unified seismic hazard modelling throughout the Mediterranean region, *Boll. Geofis. Teor. Appl.* **42**, 3–18.

Joyner, W.B. and Boore, D.M., 1981, Peak horizontal acceleration and velocity from strong-motion records including records from the 1979 Imperial Valley, California, earthquake, *Bull. Seism. Soc. Am.* **71**, 2011–2038.

Kijko, A. and Öncel, A.O., 2000, Probabilistic seismic hazard maps for the Japanese islands, *Soil Dyn. Earthquake Eng.***20**, 485–491.

Klein, F.W., Frankel, A.D., Mueller, C.S., Wesson, R.L. and Okubo, P.G., 2001, Seismic hazard in Hawaii: High rate of large earthquakes and probabilistic ground-motion maps, *Bull. Seism. Soc. Am.* **91**, 479–498.

Kulkarni, R.B., Youngs, R.R. and Coppersmith, K.J., 1984, Assessment of confidence intervals for results of seismic hazard analysis. In *Proceedings of 8th World Conference on Earthquake Engineering*, July 21–28, San Francisco, CA, Vol. 1, 263–270.

Malagnini, L. and Herrman, R.B., 2000, Ground-motion scaling in the region of the 1997 Umbria-Marche earthquake (Italy), *Bull. Seism. Soc. Am.* **90**, 1041–1051.

Malagnini, L., Akinci, A., Herrmann, R.B., Pino, N.A. and Scognamiglio, L., 2002, Characteristics of the ground-motion in Northeastern Italy, *Bull. Seism. Soc. Am.* **92**, 2186–2204.

Malagnini, L., Herrmann, R.B. and Di Bona, M., 2000, Ground-motion scaling in the Apennines (Italy), *Bull. Seism. Soc. Am.* **90**, 1062–1081.

Malagnini, L., Mayeda, K., Akinci, A. and Bragato, P.L., 2004, Estimating absolute site effects, *Bull. Seism. Soc. Am.* **94**, 1343–1352.

McGuire, R.K., 1976, FORTRAN computer program for seismic risk analysis, *US Geological Survey*, Open-File Report 76-0067, 68 pp.

Midzi, V., Hlatywayo, D.J., Chapola, L.S., Kebede, F., Atakan, K., Lombe, D.K., Turyomurugyendo, G. and Tugume, F.A., 1999, Seismic hazard assessment in Eastern and Southern Africa, *Ann. Geofis.* **42**, 1067–1083.

Minakami, T., 1974, Seismology of volcanoes in Japan. In Civetta, L., Gasparini, P., Luongo, G. and Rapolla, A. (eds), *Physical Volcanology*, Elsevier, Amsterdam: pp. 1–27.

Monachesi, G. and Stucchi, M., 1997, DOM4.1, un database di osservazioni macrosismiche di terremoti di area italiana al di sopra della soglia del danno. *Rapporto Tecnico*, GNDT, Milano-Macerata, 1052 pp. http://emidius.mi.ingv.it/DOM/home.html.

Morasca, P., Malagnini, L., Akinci, A. and Spallarossa, D., 2002, Ground-motion scaling in the Western Alps, *Seism. Res. Lett.* **73**, 251.

Munson, C.G. and Thurber, C.H., 1997, Analysis of the attenuation of strong ground-motion on the island of Hawaii., *Bull. Seism. Soc. Am.* **87**, 945–960.

Nishimura, R., Fehler, M., Baldrige, W.S., Roberts, P. and Steck, L., 1997, Heterogeneous structure around the Jemez volcanic field, New Mexico, USA, as inferred from the envelope inversion of active-experiment seismic data., *Geophys. J. Int.* **131**, 667–681.

Ordaz, M., Jara, J.M. and Singh, S.K., 1991, *Riesgo sismico y espectros de diseño en el estado de Guerrero*, Technical Report, Instituto de Ingeniería, UNAM, Mexico City, 136 pp.

Patané, D., Ferrucci, F. and Gresta, S., 1994, Spectral feature of microearthquakes in volcanic areas: Attenuation in the crust and amplitude response of the site at Mt. Etna, Italy, *Bull. Seism. Soc. Am.* **84**, 1842–1860.

Reiter, L., 1990, *Earthquake Hazard Analysis: Issues and Insights*, Columbia University Press, New York, 254 pp.

Romeo, R. and Pugliese, A., 2000, Seismicity, seismotectonics and seismic hazard of Italy, *Eng. Geol*. **55**, 241–266.

Sabetta, F. and Pugliese, A., 1987, Attenuation of peak horizontal acceleration and velocity from Italian strong-motion records, *Bull. Seism. Soc. Am.* **77**, 1491–1513.

Sabetta, F. and Pugliese, A., 1996, Estimation of response spectra and simulation of nonstationary earthquake ground-motions, *Bull. Seism. Soc. Am.* **86**, 337–352.

Sadigh, K., Chang, C.Y., Egan, J.A., Makdisi, F. and Youngs, R.R., 1997, Attenuation relationships for shallow crustal earthquakes based on California strong-motion data, *Seism. Res. Lett.* **68**, 180–189.

Scherbaum, F., Schmedes, J. and Cotton, F., 2004, On the conversion of source-to-site distance measures for extended earthquake source models, *Bull. Seism. Soc. Am.* **94**, 1053–1069, on-line material: *Distance conversion coefficients for the simulation scenarios used in this study*.

Slejko, D., Camassi, R., Cecic, I., Herak, D., Herak, M., Kociu, S., Kouskouna, V., Lapajne, J., Makropoulos, K., Meletti, C., Muço, B., Papaioannou, Ch., Peruzza, L., Rebez, A., Scandone, P., Sulstarova, E., Voulgaris, N., Živčić, M. and Zupančić, P., 1999, Seismic hazard assessment of Adria, *Ann. Geofis.* **42**, 1085–1107.

Slejko, D., Peruzza, L. and Rebez, A., 1998, The seismic hazard maps of Italy, *Ann. Geofis.* **41**, 183–214.

Tento, A., Franceschina, L. and Marcellini, A., 1992, Expected ground-motion evaluation for Italian sites. In *Proceedings of 10th World Conference on Earthquake Engineering*, 19–24 July 1992, Madrid, Spain, pp. 489–494.

Toro, G.R., Abrahamson, N.A. and Schneider, J.F., 1997, Model of strong ground motions from earthquakes in Central and Eastern North America: Best estimates and uncertainties, *Seism. Res. Lett.* **68**, 41–57.

Tromans, I.J. and Bommer, J.J., 2002, The attenuation of strong-motion peaks in Europe. In *Proceedings of 12th European Conference on Earthquake Engineering*, 9–13 September 2002, London, UK, paper no. 518.

Wells, D.L. and Coppersmith, K.J., 1994, New empirical relationships among magnitude, rupture length, rupture width, rupture area, and surface displacement, *Bull. Seism. Soc. Am.* **84**, 974–1002.

Zhang, P., Yang, Z.-X., Gupta, H.K., Bhatia, S.C. and Shedlock, K.M., 1999, Global Seismic Hazard Assessment Program (GSHAP) in continental Asia, *Ann. Geofis.* **42**, 1167–1189.